Semiclassical approach to states near potential barrier top.

V.A.Benderskii

Institute of Problems of Chemical Physics, RAS
142432 Moscow Region, Chernogolovka, Russia and
Lab. Spectrometrie Physique, UJF
BP 87, St. Martin d'Heres, Cedex, France

E.V.Vetoshkin

Institute of Problems of Chemical Physics, RAS
142432 Moscow Region, Chernogolovka, Russia

E. I. Kats

Laue-Langevin Institute, F-38042, Grenoble, France and
L. D. Landau Institute for Theoretical Physics, RAS, Moscow, Russia
(Dated: February 1, 2008)

Within the framework of the instanton approach we present analytical results for the following model problems: (i) particle penetration through a parabolic potential barrier, where the instanton solution practically coincides with the exact (quantum) one; (ii) descriptions of highly excited states in two types of anharmonic potentials: double-well X^4, and decay X^3. For the former case the instanton method reproduces accurately not only single well and double-well quantization but as well a crossover region (in the contrast with the standard WKB approach which fails to describe the crossover behavior), and for the latter case the instanton method allows to study resonance broadening and collapse phenomena. We investigate also resonance tunneling, playing a relevant role in many semiconducting devices. We show that in a broad region of energies the instanton approach gives exact (quantum) results. Applications of the method and of the results may concern the various systems in physics, chemistry and biology exhibiting double level behavior and resonance tunneling.

I. INTRODUCTION

Semiclassical mechanics has a long history. Surprisingly however some longstanding problems still exist in the theory. One of them, how to describe with a sufficient accuracy states near a potential barrier top, is the subject of our paper. It is known that the commonly used WKB method (phase integral approach) [1], [2] is reduced to matching of wave functions for classically allowed and forbidden regions. The procedure technically works for linear (or first order) turning points, and can be relatively simply performed only for one dimensional problems. However 1d problems are not of great physical importance, not only since reduced dimensionality which does not allow to model many relevant experimental situations but as well, at least partially, since 1d quantum mechanical problems can be rather easily solved numerically. Unfortunately efficency and accuracy of direct quantum mechanical numerical methods is rapidly degraded for multidimensional systems, possessing many degrees of freedom, because of the extraordinary amounts of computational work required to perform these studies. Furthermore, an extention of the WKB procedure to multidimensional systems encounters fundamental difficulties because of still unsolved matching problem for the multidimensional WKB solutions which become singular on caustic lines separating manifolds in phase space with real and imaginary momenta for each among N coordinates. Since the amount of these domains increases like $N!$, it is a tremendous task for $N > 2$. And after many decades of efforts, a complete and unifying descriptions of multidimensional WKB solutions is still not available.

The problem was first addresses a long ago, and some attempts to overcome the difficulties of the WKB approach and to improve the accuracy of the method have been performed quiet successfully. Note for example [3] where the authors have included into the standard WKB method additionally a special type of trajectories on the complex phase plane, along which the semiclassical motion is described by the Weber functions (see also [4]). However the choice of these additional special trajectories (which one has to include to improve the accuracy of the WKB method near the barrier top) depends on the detail form of the potential far from the top, and therefore for each particular case the non-universal procedure should be perform from the very beginning (see also more recent publications [5], where the authors use some distortion of Stokes diagrams, or [6], where time dependent quantum mechanical calculations for anharmonic and double-well oscillators have been performed).

Thus evidently there is some need for different from WKB semiclassical approach. One of the alternative to WKB

semiclassical formalism is so-called extreme tunneling trajectory or instanton [7], [8], [9], could be very effective for calculating globally uniform (i.e. without any singularity) wave function of the ground state. It allows to find semiclassical wave functions for a very wide class of potentials with arbitrary combinations of the first and of the second order turning points. The method recently was adapted as well for the description of low - energy excited states [10, 11]. One of the main advantage of the instanton approach that it can be readily extended for multidimensional systems using perturbative techniques (see [12] and references therein).

However before to investigate multidimensional problems, one has to study 1d potentials and 1d problems which cannot be solved accurately by the standard WKB method. It is our main concern in the paper. The generalization of the instanton procedure for highly excited states is not straightforward at all, and required additional analyses. We consider only few relatively simple examples, but such analyses are useful for gaining insight into more complex systems for which even approximate theoretical results are not available.

In fact for many interesting physical problems high accuracy calculations are out of reach by the standard WKB method but as we will see in a little while the instanton approach is afford to overcome the difficulties of the WKB procedure. Since this fact has largely gone unnoticed in the previous studies, we found it worthwhile to present the investigation of a few simple examples in a short and explicit form, and also to point out its practical usability. And besides the study (apart from the aim to illustrate the efficency of the instanton approach) is a prerequisite for an explanation and successful description of many relevant physical phenomena (e.g. low-temperature quantum kinetics of phase transitions, see e.g. [13]) where an active (reaction) path is confined effectively to one dimension.

All examples considered in our paper, related to the fundamental problems of chemical dynamics and molecular spectroscopy (see e.g. the monography [9] and references herein). Symmetric or slightly asymmetric double-well potentials are characteristic for molecules and Van der Waals complexes with more than one stable configurations [14], [15], [16], [17]. The states of such systems close to the barrier top (theoretically described by the instanton approach in our paper) are most relevant for radiationless evolution of highly excited states. These states have a double nature (localized - delocalized) and the nature manifests itself in the form of wave functions which contain simultaneously the both components: localized in one from the wells, and delocalized between the both of the wells. The states close to the barrier top of decay potentials govern of thermally activated over-barrier transition amplitudes. For the low energy states the main reduction factor is the tunneling exponent, while the contribution of the highly excited states is limited by the Boltzmann factor. Our instanton calculations demonstrate that there is no sharp boundary between quasistationary and delocalized states. Recently two of us (V.B. and E.K.) [18] investigated the eigenstates of the highly asymmetric double well potential. We have shown that quantum irreversibility phenomena occur when the spacing between neighbouring levels of a deeper well becomes smaller than the typical transition matrix element. Obviously this criterion can be also applied to the states near the barrier top. Note that for the low energy states the asymmetry providing irreversible behavior should be very large, whereas for the states near the barrier top, the condition to have the ergodic behavior is not so severe, it is sufficient that the asymmetry of the potential is comparable to the barrier height.

Our paper has the following structure. Section II contains basic equations of the instanton method necessary for our investigation. As an illustration of the method we consider a touchstone quantum mechanical problem - penetration of a particle through parabolic potential barrier. In this case the instanton solutions which are the asymptotics of the Weber equation are exact. Section III is devoted to the investigation of highly excited states in a double - well potential. For sake of concreteness and simplicity we study a quartic anharmonic X^4 potential. The instanton approach allows us to reproduce accurately not only asymptotic behavior but also a crossover region from single well to double wells quantization. In the section IV analogous problem for X^3 anharmonic potential is studied. Section V is devoted to so-called resonance tunneling phenomena, interesting not only in its own right but as well playing a relevant role in many semiconducting double barrier structures. Finally, in the section VI we discussed the results and conclude. In the Appendix to the paper we compute so-called connection matrices, which provide a very efficient method of finding semiclassical solutions to the Schrodinger equation in potentials having several turning points. It is important and significant to know the connection matrices. This is not only in itself but also for developing good analytical approximation. Those readers who are not very interested in mathematical derivation can skip the Appendix and find all the results in the main body of the paper.

II. PENETRATION THROUGH PARABOLIC POTENTIAL BARRIER.

A. Instanton approach.

Let us remind for the sake of conveniency the main ideas of the instanton approach. The first step of the approach derived in [7] and [8] is so-called Wick rotation of a phase space corresponding to a transformation to imaginary time $t \to it$. At the transformation potential and kinetic energy change their signs, and Lagrangian is replaced by

Hamiltonian in the classical equation of motion. After this Wick rotation the standard oscillating WKB wave functions are transformed into decaying exponentially functions which are vanished at $X \to \pm\infty$. Following to [10], [11] we will use slightly different formulation of the instanton method, from the very beginning assuming exponentially decaying real-valued wave functions. Thus taking into account that the wave functions of bound states can be chosen as real quantities, one can look for a solution to the Schrodinger equation in the form

$$\Psi = \exp\left(-\gamma\sigma(X)\right), \tag{2.1}$$

where γ is semiclassical parameter($\gamma \equiv m\Omega_0 a_0^2/\hbar$, where m is a mass of a particle, a_0 is a characteristic length of the problem, e.g. the tunneling distance, Ω_0 is a characteristic frequency, e.g. the oscillation frequency around the potential minimum, and further we will set $\hbar = 1$ measuring energies in the units of frequency) which is assumed to be sufficiently large, and σ can be called an action and for this function the first order differential equation of the Ricatti type should hold

$$\gamma^2 \left[-\frac{1}{2}\left(\frac{d\sigma}{dX}\right)^2 + V(X) \right] + \gamma\left[\frac{1}{2}\frac{d^2\sigma}{dX^2} - E \right] = 0, \tag{2.2}$$

where $V(X)$ is a potential, and ϵ gives particle eigen states (energies). Here and below we use dimensionless variables (for the energy $\epsilon = E/\Omega_0$, for the potential $V = U/\gamma\Omega_0$, and for the coordinate $X = x/a_0$, where E and U are corresponding dimensional values for the energy and for the potential). We believe that $\gamma \gg 1$ and therefore $\sigma(X)$ can be expanded into the asymptotic series

$$\sigma(X) = W(X) + \gamma^{-1}W_1(X) + \gamma^{-2}W_2(X) + \dots. \tag{2.3}$$

The first and the second over γ^{-1} order terms become identically zero, if the time independent Hamilton-Jacobi equation (HJE) and so-called transport equation (TE) are satisfied

$$\frac{1}{2}\left(\frac{dW}{dX}\right)^2 = V(X), \tag{2.4}$$

and

$$\frac{dW}{dX}\frac{dA}{dX} + \frac{1}{2}\frac{d^2W}{dX^2}A = \epsilon A, \tag{2.5}$$

where

$$A(X) \equiv \exp(-W_1(X)). \tag{2.6}$$

The essential advantage of the instanton method in comparison to a standard WKB is that in the former approach HJE is solved at $E = 0$, and therefore the classically allowed regions disappear. A price we should pay for the advantage is an appearance of second order turning points (unlike WKB method where there are only linear turning points).

It is well known that WKB wave functions are singular at the turning points, and therefore different approximations represent the same wave function in various domains. The famous Stokes phenomenom [2] is related to the distribution of the turning points, and Stokes and anti-Stokes lines emanate from each turning point. By the definition Stokes lines represent the lines where the dominance of the dominant exponential semiclassical solution to the Schrodinger equation becomes strongest, and anti-Stokes lines, on the other hand represent the lines across which the dominance and subdominance of the solutions interchange. Evidently near Stokes and anti-Stokes lines the WKB approximation does not work and should be refine [2]. On the contrary, since classically accessible regions do not exist within the instanton formalism, the Stokes lines pass continously through second order turning points, and globally uniform real solutions to the Schrodinger equation can be constructed using the asymptotically smooth transformation of the instanton wave functions into the Weber functions. Just this global uniformity is the principal advantage of the instanton method.

A clearer idea of the instanton approach is obtained by the derivation of well known [1] quantization rules for the harmonic oscillator ($V(X) = X^2/2$). For a given energy ϵ any solution of the Schrodinger equation can be represented as a linear combination of the solutions of the Weber equation [22]

$$\frac{d^2\Psi}{dz^2} + \left(\nu + \frac{1}{2} - \frac{z^2}{4}\right)\Psi(z) = 0, \tag{2.7}$$

where $z \equiv X\sqrt{\gamma}$, and $\nu = \epsilon - 1/2$. The basic solutions of (2.7) are the parabolic cylinder functions [22], and only the function $D_\nu(-z)$ is vanished at $z \to \infty$ for $arg z = 0$. For the $arg z = \pi$ the asymptotic behavior of this function at $z \to \infty$ is given by [22]

$$D_\nu(-z) = z^\nu \exp -\left(\frac{z^2}{4}\right) - \frac{\sqrt{2}\pi}{\Gamma(-\nu)} \exp(i\pi\nu) z^{-\nu-1} \exp\left(\frac{z^2}{4}\right), \qquad (2.8)$$

It can vanish at $z \to \infty$ only at the poles of $\Gamma(-\nu)$, and this condition gives the exact eigenvalues of the harmonic oscillator

$$\epsilon = n + \frac{1}{2}.$$

Moreover since $D_\nu(-z)$ for integer and positive ν coincide with known harmonic oscillator eigenfunctions [1], the instanton approach is exact for the harmonic oscillator.

B. Tunneling through the harmonic barrier.

For the next less trivial illustration of the instanton approach efficiency, let us apply the method to the problem of quantum mechanical tunneling through a parabolic potential

$$U(x) = U_0 - \frac{m\Omega_0^2}{2}x^2, \qquad (2.9)$$

where m is a mass of a tunneling particle, and Ω_0 is a characteristic frequency (curvature of the potential). Besides the potential has a characteristic space scale a_0. Using Ω_0 and a_0 to set corresponding scales the parabolic potential (2.9) can be written in the following dimensionless form

$$V(X) = V_0 - \frac{1}{2}X^2. \qquad (2.10)$$

The Schrodinger equation in these variables

$$\frac{d^2\Psi}{dX^2} + [\gamma^2 X^2 - \alpha\gamma]\Psi(X) = 0, \qquad (2.11)$$

where

$$\alpha = 2\frac{U_0 - E}{\Omega_0}, \qquad (2.12)$$

and introduced above semiclassical parameter $\gamma \gg 1$.

The Schrodinger equation (2.11) can be transformed into the Weber equation [22] by $\pi/4$ rotation in the complex plane X

$$X = \frac{1}{\sqrt{2\gamma}} z \exp\left(\frac{i\pi}{4}\right),$$

and therefore the solution of (2.11) can be represented as a linear combination of the parabolic cylinder functions D_ν [22]

$$\Psi_\nu(z) = c_1 D_\nu(z) + c_2 D_\nu(-z), \qquad (2.13)$$

where $\nu = -(1/2) - i(\alpha/2)$.

At $X \to \infty$ only the transmitted wave exists with the amplitude (i.e. transmission coefficient) T

$$\Psi \simeq T \exp \frac{i\gamma X^2}{2}, \qquad (2.14)$$

while for $X \to -\infty$ one has the incident ($\propto \exp(-i\gamma X^2/2)$) and the reflected wave $\propto R\exp(i\gamma X^2/2)$. By a standard quantum mechanical procedure [1] the transmission T and the reflection R coefficients can be found using known

asymptotics of the parabolic cylinder functions [22] at the fixed energy (i.e. at the fixed α) and it leads to a well known [1] expression

$$|T|^2 = \frac{1}{1 + \exp(\pi\alpha)} \,. \tag{2.15}$$

Note that the solutions (2.13) are the exact solutions to the Schrodinger equation in the parabolic potential (2.10). Now let us apply to the same problem the instanton approach shortly described above. The solutions of HJE (2.4) and TE (2.5) equations which are milestones of the method can be found strait-forward and read

$$W = \pm i\frac{X^2}{2} \,,\; A = A_0 X^{-1/2} \exp(\pm i\alpha \ln X/2) \,, \tag{2.16}$$

where the integration constant A_0 determines energy dependent phases of the wave functions. From the comparison of (2.16) and (2.13) one can see that the instanton wave functions are the asymptotics of the parabolic cylinder functions, and, therefore, since the transmission T and reflection R coefficients are determined only by the asymptotic behavior, the values of T and R found in the frame work of the instanton approach coincide with the exact quantum mechanical ones at any value of the energy (of the parameter α). Let us remind that the instanton and exact quantum mechanical solutions for the harmonic oscillator also coincide for any energy.

To accomplish this subsection and for the sake of the skeptical reader it is worth to mention that the WKB wave functions coincide with the exact solutions only at $\alpha \ll -1$. In the region $|\alpha| \leq 1$, i.e. when characteristic size of the forbidden region becomes comparable with the particle wave length, specific interference phenomena between transmitted and reflected waves occur, and this kind of phenomena can not be reproduced in the standard WKB approach assuming that all turning points are independent ones.

As an illustration in Fig. 1 we show energetical (α) dependence of the phase for the wave function reflected by the parabolic potential. The exact quantum mechanical and the instanton solutions (ϕ_0 in Fig. 1) are indistinguishable over a broad region of energies, while the WKB solution (ϕ_0^{WKB} in Fig. 1) is deviated from both of them.

C. Connection matrices.

Our analysis can be brought into a more elegant form by introducing so-called connection matrices. In the instanton approach (as in any semiclassical treatment of the scattering or of the transition processes) we are only concerned with the asymptotic solutions and their connections on the complex coordinate plane. Thus it is important and significant to know the connection matrices. These connection matrices provide a very efficient method of finding semiclassical solutions to the Schrodinger equation in potentials having several turning points. This is a relevant starting point also for developing good analytical approximation.

It is convenient to formulate the general procedure for calculating of the connection matrices for an arbitrary combinations of the first and of the second order turning points. After that the procedure can be applied to any particular problem under investigation. To do it technically, one has to extend the known for linear turning points procedure [2]. All necessary details of the generalization are given in the Appendix to the paper, and here we present only main definitions and results. For the equation

$$\frac{d^2\Psi}{dz^2} + \gamma^2 q(z)\Psi(z) = 0 \,, \tag{2.17}$$

in the semiclassical limit $\gamma \gg 1$ the Stokes and anti-Stokes lines are determined by the following conditions, respectively

$$ReW(z) = 0 \,, \tag{2.18}$$

and

$$ImW(z) = 0 \,, \tag{2.19}$$

where

$$W(z) = \int_{z_0}^{z} \sqrt{q(z)}dz \,, \tag{2.20}$$

where z_0 is the turning point under consideration.

For the harmonic potential we have only the linear turning points for real (at $\alpha > 0$) and imaginary (at $\alpha < 0$) energies. In the Appendix we calculated all the connection matrices we need. Thus to fully analyze the problem for the whole range of parameters, we should know only the distributions of turning points and Stokes and anti-Stokes lines on the complex plane. At real turning points ($\alpha > 0$) $X_{1,2} = \pm(\alpha/\gamma)^{1/2}$, there are 4 Stokes and 4 anti-Stokes lines, and two cuts on the complex plane (see Fig. 2).

At $\alpha \gg 1$ the connection matrix can be easily calculated as the direct product of the connection matrices found in the Appendix ($\hat{M}^-$ from (A5) and the Hermitian conjugated matrix $\hat{M}^+$) and the following diagonal shift matrix

$$\begin{pmatrix} \exp(\pi\alpha/2) & 0 \\ 0 & \exp(-\pi\alpha/2) \end{pmatrix} \tag{2.21}$$

It leads to the transmission coefficient $T \simeq \exp(-\pi\alpha/2)$, i.e. coinciding with (2.15) in the limit $\alpha \gg 1$ with the exponential accuracy. To improve the accuracy at smaller values of α, at the calculation of the connection matrices, one must take into account not only the contributions from the contours going around the turning points, but as well the additional contribution to the action from the closed path (with a radius $\gg |X_{1,2}|$) going around the both points $X_{1,2}$ (see Fig.2). The procedure changes the Stokes constant T_3 (on the dashed line separating the regions 3 and 4 in Fig. 2), which becomes

$$|T_3| = [1 + \exp(-\pi\alpha)]^{1/2},$$

and finally it leads to the correct transmission coefficient

$$T = iT_3^{-1} \exp\left(-\frac{\pi\alpha}{2}\right),$$

which is identical to (2.15).

In the case $\alpha < 0$, the whole picture (see Fig. 3) of the Stokes and of the anti-Stokes lines and turning points, is turned by the angle $\pi/2$ with respect to depicted in Fig. 2. If one bluntly takes the point $X = 0$ as the low integration limit for the action W^* (A11), it leads to the following transmission coefficient

$$T = 1 - \frac{1}{2}\exp(-\pi|\alpha|),$$

which can be reliable (with the accuracy $\exp(-2\pi|\alpha|)$) only for $|\alpha \gg 1$. Again as we did for $\alpha > 0$ case, to improve the accuracy we should take into account the contribution from the path surrounding the both imaginary turning points (this fact was noticed long ago by Pokrovskii and Khalatnikov [3]).

At the isolated linear imaginary turning point iX_1 the connection matrix is found from (A5)

$$\tilde{M}_1^+ = \begin{pmatrix} 1 & i\exp(-\pi|\alpha|/2) \\ 0 & 1 \end{pmatrix} \tag{2.22}$$

Analogously the Hermitian conjugated matrix $\tilde{M}_1^-$ comes from the contribution from the closed path surrounding $-iX_1$. These contours provide only the amplitude of the dominant (exponentially increasing) wave. However the accuracy is not enough to find the amplitude of the corresponding subdominant solution (exponentially decaying wave function), and thus it leads wrongly to the transmission coefficient $T = 1$. To improve the accuracy and to find correctly T, one should include to the procedure the connection matrix for the isolated second order turning point (which is in this particular example, the maximum of the potential). Using (A9) we can find explicitly this matrix

$$\tilde{M}_2 = \begin{pmatrix} (1 + \exp(-\pi|\alpha|))^{1/2} & i\exp(-\pi|\alpha|/2) \\ -i\exp(-\pi|\alpha|/2) & (1 + \exp(-\pi|\alpha|))^{1/2} \end{pmatrix} \tag{2.23}$$

In principle the same kind of calculations might be performed in the adiabatic perturbation theory (which employs in fact the Plank constant smallness equivalent to $\gamma \gg 1$). Note for example the paper [21] where the contributions from the contours surrounding turning points (analogous to presented above) have been taking into account. It seems very plausible that on this way one will be able to combine the instanton approach and the adiabatic perturbation theory, however, this issue is beyond the scope of our paper and will be discussed elsewhere.

III.   HIGHLY EXCITED STATES IN DOUBLE - WELL POTENTIAL

Literally, the instanton approach described in the previous section, is valid for the states with characteristic energies which are small in comparison to the barrier height. However as we will show in this section the instanton method

works pretty good for the energy states near the barrier top V_0. As an illustration let us consider symmetric double well potential (quartic anharmonic X^4 potential)

$$V_0 - V(X) = \frac{1}{2}X^2(1 - X^2).\tag{3.1}$$

The Schrodinger equation with the potential (3.1) can be rewritten in dimensionless variables in the following form most convenient for the application of the instanton approach

$$\frac{d^2\Psi}{dX^2} + [2\gamma^2(V_0 - V(X)) - \alpha\gamma]\Psi(X) = 0.\tag{3.2}$$

Furthermore HJE and TE instanton equations are correspondingly

$$\frac{1}{2}\left(\frac{dW}{dX}\right)^2 = V_0 - V(X),\tag{3.3}$$

and

$$\frac{dW}{dX}\frac{dA}{dX} + \frac{1}{2}\left(\frac{d^2W}{dX^2} + i\alpha\right)A = 0.\tag{3.4}$$

Formal solutions to this set of equations (3.3 - 3.4) are even and odd instanton wave functions

$$\Psi_I^\pm = A_\pm(X)\exp(i\gamma W_\pm(X)),\tag{3.5}$$

where the action $W_\pm$ (solution of HJE) should be determined from

$$\frac{dW_\pm}{dX} = \pm\sqrt{2(V_0 - V(X))},\tag{3.6}$$

and the amplitude (pre-factor) in own turn reads as

$$A_\pm = \left|\frac{dW_\pm}{dX}\right|^{-1/2}\exp\left(-i\alpha\int\left(\frac{dW_\pm}{dX}\right)^{-1}dX\right).\tag{3.7}$$

The quantization rules [1] are related to continuous matching of the solutions at the turning points (the second order turning point $X = 0$, and the linear turning points $X = \pm 1$ for $\alpha > 0$ and $X = \pm i$ for $\alpha < 0$). The crucial advantage of the instanton solutions (3.5) is due to the fact that these functions have no singularities at all inside the barrier, since the corresponding exponents are pure imaginary ones in the classically accessible regions (unlike WKB solutions). Besides the general form of the instanton wave functions does not depend noticeably on whether $E < V_0$ or $E > V_0$. This advantage allows us to include the instanton wave functions into the basis of globally uniform functions diagonalizing the Hamiltonian even for highly excited states.

   The described above general procedure for searching instanton solutions to the Schrodinger equation with the model potential (3.1) has a tricky point, what is the motivation for presenting in some details below the explicit procedure for the search, and new results will be emanated from our investigation. The procedure includes several steps:

- Near the second order turning point one can use the exact solution to the Schrodinger equation (2.14) with $c_1 = \pm c_2$ for the even and odd solutions respectively. For $|X| \gg 1$ from (2.14) and known asymptotics of the parabolic cylinder functions [22]

$$\Psi(X) = \frac{c_1}{\sqrt{X}}\left[\frac{\exp(if(X))}{\Gamma((1 - i\alpha)/4)} + \frac{\exp(-if(X))}{\Gamma((1 + i\alpha)/4)}\right],\tag{3.8}$$

   where

$$c_1 = -\frac{2\pi}{\Gamma((3 + i\alpha)/4)}\exp\left(-\frac{\pi\alpha}{8}\right)2^{-i\alpha/4}(2\gamma)^{-1/4},\tag{3.9}$$

   and

$$f(X) = \frac{\gamma}{2}X^2 - \frac{\alpha}{2}\ln X - \frac{\alpha}{4}\ln\gamma - \frac{\pi}{8}.\tag{3.10}$$

   To have correct even and odd linear combinations conforming to (3.5)

$$c_\pm = c_1\frac{\exp(\pm if_1)}{\Gamma((1 \pm i\alpha/\sqrt{2})/4)},\tag{3.11}$$

   where $f_1 = (\alpha\ln\gamma)/4 + \pi/8$.

- Near the linear turning point $X = \pm 1$, the Schrodinger equation is reduced to the Airy equation [22]

$$\frac{d^2\Psi}{dy^2} - y\Psi(y) = 0\,,\tag{3.12}$$

where at $X < 0$

$$y = \gamma^{2/3}\left|X + 1 + \frac{\alpha}{\gamma}\right|\,.\tag{3.13}$$

The solution vanishing at $y \to \infty$ is [22]

$$\Psi(y) = |y|^{-1/4}\sin\left(\frac{2}{3}|y|^{3/2} + \frac{\pi}{4}\right)\,.\tag{3.14}$$

Continuing this solution into the regions $(X \pm 1)\sqrt{2\gamma} \gg 1$ and sewing there with (3.8) we come to

$$\frac{c_+}{c_-} = \exp\left(-i2\gamma W^* + i\frac{3\pi}{2}\right)\,,\tag{3.15}$$

where W^* is the energy dependent action in the interval $[X = 0\,, X = 1]$.

- Comparing (3.15) and (3.11) we find the quantization rules which read for the even states as

$$\frac{\Gamma\left((1 + i\alpha)/4\right)}{\Gamma\left((1 - i\alpha)/4\right)} = \exp\left(-2i\gamma W^* - i\frac{3\pi}{2}\right)\,,\tag{3.16}$$

and for the odd states as

$$\frac{\Gamma\left((3 + i\alpha)/4\right)}{\Gamma\left((3 - i\alpha)/4\right)} = \exp\left(-2i\gamma W^* - i\pi\right)\,.\tag{3.17}$$

- Finally from (3.16), (3.17) we come to the quantization rule which can be written in the single form for the both, even and odd, states

$$2\gamma W^* + 2\phi(\alpha) \equiv \left(\begin{array}{c} (5\pi/4) + 2\pi n - \arctan(th\,(\pi\alpha/4)) \\ (3\pi/4) + 2\pi n - 2\arctan(th\,(\pi\alpha/4)) \end{array}\right)\,.\tag{3.18}$$

The relation (3.18) is the quantization rule we looked for, and which allows us now to pick the fruits of the instanton method. For the highly excited states, i.e. $\alpha \ll -1$ one can find from (3.18)

$$2\gamma W^* + 2\phi(\alpha) = \pi\left(n + \frac{1}{2}\right)\,,$$

where n is an integer number. For the low-energy states $\alpha \gg 1$ (3.18) reproduces the known quantization rule

$$\gamma W_L^* = \pi\left(n + \frac{1}{2}\right) \pm \frac{1}{2}\exp\left(-\frac{\pi\alpha}{4}\right)\,,$$

where W_L^* is the action in the classically admissible region between linear turning point in the left well, namely

$$\gamma W_L^* = \gamma W^* + \phi(\alpha)\,.\tag{3.19}$$

Note the essential advantage of the instanton quantization rule (3.18) with respect to the traditional WKB formalizm, where the quantization rules in tunneling and over-barrier regions are completely different [1]. The instanton approach gives the single quantization rule (3.18) which is valid in the both regions and besides fairly accurate describes the crossover behavior near the barrier top, where periodic orbits localized at separate wells transform into a common figure height orbit enclosing the both wells.

We illustrate the results of this section in the Fig. 4, where the universal dependence of the eigen values (in the symmetric double - well potential (3.1) on α is plotted. For the sake of comparison we presented in the same figure the eigen values found by the conventional WKB procedure and by the exact quantum mechanical computation. It is

clear from the figure that the WKB method errors are maximal in the region of small $|\alpha|$, since the oscillation period diverges logarithmically in this region (the particle spends infinitely long time near the second order turning point). On the contrary, the errors of the instanton approach are minimal near the barrier top (small $|\alpha|$).

As we already mentioned at the beginning of this section, near the potential minimum, the instanton approach also works very accurate. Generally speaking the instanton solutions are always correct when the deviation from the corresponding minimum exceeds characteristic zero - point amplitudes. Mathematically the accuracy of the instanton approach is based on the transformation of the semiclassical solutions into the harmonic oscillator eigenfunctions (what ensures as well the correct normalization of the instanton wave functions). Therefore it is naturally to expect that the instanton method works very accurate near the barrier top and near the potential minimum. On the contrary, the intermediate region, where anharmonic shape of the potential is relevant, one should expect a poor accuracy of the instanton method. Fortunately it turns out that the mathematical nature of the problem is on our side, and the instanton approach has a reasonable accuracy (of the order of the accuracy of the WKB method) even in this region. The fact is that the instanton wave functions are exact not only in zero but in the first order over anharmonic corrections to the potential approximation. It can be shown using anharmonic perturbative procedure proposed by Avilov and Iordanskii for WKB functions [19] and generalized in [20] for the instanton wave functions.

Besides, what is more relevant for practical computations, the instanton wave functions (unlike WKB ones) are continuous near its "own" minimum. Numerical estimations show that in the intermediate energetical region, the accuracy of the instanton wave functions is of the order of $5-10\%$.

To accomplish the section we present the connection matrices needed to find semiclassical solutions to the Schrodinger equation in the double - well potential. Analogously to the results of the Section II, the connection matrix for the instanton solutions is the product of the connection matrices (A5) for the linear turning points, and the connection matrix for the second order turning point, which is for the case under consideration, the maximum of the double - well potential. Using (A9) one can find for this latter connection matrix

$$
\begin{pmatrix}
2(\exp(\pi\alpha/2) + (1 + \exp(\pi\alpha))^{1/2}\cos(2\gamma W^*)) \\
(1 + \exp(\pi\alpha))^{1/2}\sin(2\gamma W^*)
\end{pmatrix}
\tag{3.20}
$$

$$
\begin{pmatrix}
-(1 + \exp(\pi\alpha))^{1/2}\sin(2\gamma W^*) \\
(1/2)(-\exp(\pi\alpha/2) + (1 + \exp(\pi\alpha))^{1/2}\cos(2\gamma W^*))
\end{pmatrix}
$$

It is worth to note that the reflected wave near the barrier top acquires non trivial phase factor. The phenomenom is related to interference of incident, reflected and transmitted waves, and thus the phase has some geometrical meaning, like famous Berry phase [23]. The geometrical origin of the phase manifests itself more clearly if we remind that the semiclassical phase factor is determined by the probability density flow through the barrier

$$
J = i\Psi^* \frac{d\Psi}{dX} \, .
$$

One can look to this phase factor from a slightly different point of view, since tunneling results in the phase shift related to the change of eigenvalues. The quantization rules (3.18), (3.19) can be rewritten in the following form, which is the definition of eigenvalues ϵ_n:

$$
\epsilon_n = n + \frac{1}{2} + \chi_n \, ,
$$

where n is integer numbers numerating eigenvalues, and χ_n is determined by an exponentially small phase shift due to the existence of the barrier between two wells. The phase shift χ_n has the same functional form (and physical meaning) as the geometrical phase factor (appearing due to interference phenomena) which a quantum mechanical wave function acquires upon a cyclic evolution [23], [24], [25].

IV. DECAY POTENTIAL

In this section we present theoretical studies of highly excited states in a decay potential, which for definiteness will be chosen as anharmonic X^3 potential

$$
V_0 - V(X) = \frac{1}{2}X^2(1 - X) \, .
\tag{4.1}
$$

As a first (but compulsory) step we investigate the low - lying tunneling states.

A. Tunneling decay of metastable states.

We start from this simple case to pick first the low-hanging fruits, i.e. to describes states

$$V_0 \gg \epsilon_n \gg V(X \to \infty), \tag{4.2}$$

what means that a local minimum is separated from continuum spectrum by a high energetical barrier, and therefore the quasistationary states ϵ_n are characterized by "good" quantum numbers n. Note that a generic decay potential, depicted in Fig. 5, is determined by the positions of the barrier top X_0 and three turning points $-X_1$, $X = 0$, $+X_2$, and near these points

$$V(X) = \left\{ \begin{array}{c} V_0 - (dV/dX)_{X=-X_1} (X + X_1), \, |X + X_1| \to 0 \\ \frac{1}{2}X^2, \, |X| \to 0 \\ V_0 - \frac{1}{2}(X - X_0)^2, \, |X - X_0| \to 0 \\ -(dV/dX)_{X=X_2} (X - X_2), \, |X - X_2| \to 0 \end{array} \right\}. \tag{4.3}$$

The potential (4.1) is just a particular example of the generic decay potential (4.3) ($X_1 = 1/3$, $X_0 = 2/3$, $X_2 = 1$, and $V_0 = 2/27$) which we will use only for the sake of concreteness and explicit illustration, all presented below results are equally valid for the generic potential. As a note of caution we should also remark that in the instanton approach to this problem we always have deal with the only two turning points. For the low energy states the points are X_2 and the potential minimum $X = 0$, for the high energy states the points are $-X_1$ and the potential maximum X_0.

According to (4.1) there are no turning points at $X > X_2$, and at $X \gg X_2$ the potential can be considered as a constant, and therefore the wave functions asymptotically at $X \gg X_2$ should coincide with plane waves. Furthermore near the linear turning point $X = 1$ the Schrodinger equation with X^3 anharmonic potential (4.1) is reduced to the Airy equation (3.12), whose solutions are linear combinations of the indices $\pm 1/3$ Bessel functions at real (for $X < 1$) and imaginary (for $X > 1$) values of the arguments

$$\Psi(u) = \sqrt{u} \left[B_+ I_{1/3} \left(\frac{2u^{3/2}}{3} \right) + B_- I_{-1/3} \left(\frac{2u^{3/2}}{3} \right) \right], \tag{4.4}$$

and

$$\Psi(\zeta) = \sqrt{\zeta} \left[-B_+ J_{1/3} \left(\frac{2\zeta^{3/2}}{3} \right) + B_- J_{-1/3} \left(\frac{2\zeta^{3/2}}{3} \right) \right], \tag{4.5}$$

where

$$u = (2\gamma)^{2/3} \left[1 - X - \frac{\nu + (1/2)}{\gamma} \right], \tag{4.6}$$

at $X < 1$, and

$$\zeta = (2\gamma)^{2/3} \left[X - 1 + \frac{\nu + (1/2)}{\gamma} \right], \tag{4.7}$$

at $X > 1$ (remind that here $\nu = \epsilon_n - 1/2$).

The coefficients $B_\pm$ must be chosen such a manner that at $\zeta \gg 1$ (4.5) gives the plane waves, and thus using known asymptotics of Bessel functions [22]

$$B_+ = B_- \exp\left(-i\frac{\pi}{3} \right).$$

In the classically forbidden region $u \gg 1$ the instanton solutions of HJE (2.4) and TE (2.5) matching continuously near the turning points the quantum mechanical solutions of the Schrodinger equation is

$$\Psi_\pm = A_\pm \exp(\pm \gamma W), \tag{4.8}$$

where

$$A_\pm = X^{-1/2}(1 - X)^{-1/4} \left[\frac{1 - \sqrt{1 - X}}{1 + \sqrt{1 - X}} \right]^{-\epsilon_n}, \tag{4.9}$$

and

$$W = \frac{8}{15} - \frac{4}{3}(1 - X)^{3/2} + \frac{4}{5}(1 - X)^{5/2}. \tag{4.10}$$

The wave functions of the quasistationary states, we are looking for, are the linear combinations of the instanton solutions (4.8) and the suitable coefficients in the combinations are determined from the condition of asymptotically matching to the parabolic cylinder (2.13) and Airy functions, what leads to the following equation for complex eigen values ν

$$-\frac{\sqrt{2\pi}}{\Gamma(-\nu)} \exp\left(\frac{16}{15}\gamma\right) = i\gamma^{\nu+(1/2)}2^{6\nu+3}. \tag{4.11}$$

Since the function $\Gamma(z)$ has a simple first order pole at $z = -n$, one can easily find the main contribution to the decay rate Γ_n of the quasistationary state ϵ_n

$$\frac{\Gamma_n}{\Omega_0} = \sqrt{\frac{2}{\pi}} \frac{\gamma^{\nu+1/2}2^{6\nu+3}}{n!} \exp\left(\frac{16}{15}\gamma\right). \tag{4.12}$$

Note that for the ground state $n = 0$ (4.12) coincides to the result found by Caldeira and Legget [26]. From the other hand the decay rate is related to the current flow [1] at $X \to +\infty$ providing the constant amplitude of the outgoing wave

$$\frac{\Gamma_n}{\Omega_0} = \left(2i\sqrt{\gamma}\int |\Psi|^2 dX\right)^{-1}\left[-\Psi^*\frac{d\Psi}{dX} + \Psi\frac{d\Psi^*}{dX}\right]. \tag{4.13}$$

Introducing into (4.13) the explicit form of the wave functions (4.5), (4.6), (4.7) we get

$$\frac{\Gamma_n}{\Omega_0} = \frac{9}{8}\frac{\gamma^{1/6}}{2^{1/3}}|B_+|^2, \tag{4.14}$$

which is equivalent to (4.13).

The decay rate according to (4.14) depends only on the normalization of the instanton wave function and on the amplitude of the outgoing wave. The both characteristics are determined essentially by the behavior of the instanton wave function in the vicinity of the turning points only. Note however that in this approximation the instanton computation of the decay rate (4.13) or (4.14) is satisfactory one only for the ground state, because corrections of the order of γ^{-1} strongly increase with the quantum number n. This sins of omission can be easily relaxed if we take into account the X^3 anharmonic contribution into the potential as a perturbation

$$\frac{\Gamma_n}{\Omega_0} = \sqrt{\frac{2}{\pi}} \frac{\gamma^{\nu+1/2}2^{6\nu+3}}{n!} \exp\left(\frac{16}{15}\gamma\right)\left[1 - \frac{1}{576\gamma}(164n^3 + 246n^2 + 1216n + 567)\right]. \tag{4.15}$$

The decay rate calculated according to (4.15) provides the same level of the accuracy as the WKB and exact quantum mechanical computations for $\gamma \geq 5$. Out of the regime of interest, the instanton theory loses all pretence of predictability.

B. Highly excited states for anharmonic X^3 potential.

In the Subsection IV A we calculated the decay rate of low-energy metastable states. For this case (the states ϵ_n can be characterized by the good quantum number n) period of oscillations in the well is smaller than inverse decay rate ($\epsilon_n \gg \Gamma_n/\Omega_0$), and Γ_n is determined by the probability current density flowing from the well into the classically admissible region ($X > X_0$ for a given energy ϵ_n, see Fig. 5 and notations herein) at the condition of vanishing back-flow from this region to the barrier. Evidently the method does not work for highly excited states, when $\Gamma_n \geq \epsilon_n\Omega_0$. In this Subsection we go one step further with respect to the Subsection IV A extending the instanton approach to the decay of highly excited states.

First it is worth noting that the wave functions must be vanished at $X \to -\infty$, and besides could be always chosen as real - valued quantities at $X \to +\infty$. From these two conditions one can find the relations between the instanton wave functions in the regions $X < X_1$ and $X > X_0$ (see notations in Fig. 5), and, as a result of these relations, to calculate the phase $\delta(\alpha)$ (counted from the barrier top) of the standing wave in the region $X > X_0$. It reads

$$\exp(i2\delta) = -i\exp(-i2\gamma W^*)\frac{1 + \sqrt{2\pi}\exp(-\pi\alpha/4)\exp(i2\gamma W^*)[\Gamma(1 - i\alpha/2)]^{-1}}{1 + \sqrt{2\pi}\exp(-\pi\alpha/4)\exp(-i2\gamma W^*)[\Gamma(1 + i\alpha/2)]^{-1}}. \tag{4.16}$$

According to the standard quantum mechanics [1] the phase (4.16) determines the scattering amplitude. Thus from (4.16) we can find the scattering amplitude in the deep classically forbidden region, and as a result of it to compute the eigen values in this region. To perform the calculation we need to know the terms of the order of $\exp(-\pi|\alpha|)$ in the Γ-functions expansion (which are beyond the standard Stirling formula) [22]

$$\Gamma\left(\frac{1 \pm i\alpha}{2}\right) \simeq \sqrt{2\pi}\exp\left(-\frac{\pi\alpha}{4} \pm i\phi\right)\left(1 - \frac{1}{2}\exp(-\pi|\alpha|)\right), \tag{4.17}$$

where

$$\phi(\alpha) \equiv \frac{\alpha}{2}\left[\ln\frac{|\alpha|}{2} - 1\right]. \tag{4.18}$$

Finally from (4.16), and taking into account (4.17), (4.18) we find (with required exponential accuracy) the poles of the scattering amplitude

$$2\gamma W_L^* = 2\gamma W^* + \phi(\alpha) = \pi(2n+1) - i\left[\frac{\pi}{4}(|\alpha| - \alpha) + \frac{1}{2}\exp(-\pi|\alpha|)\right], \tag{4.19}$$

and therefore explicitely solving (4.19), the complex eigen values, and in particularly the decay rate for highly excited states in the anharmonic decay potential.

The same manner as for low energy tunneling states, for highly excited states (i.e. at $|\alpha| \gg 1$) the real part of the eigen values ϵ_n is determined by the action along closed trajectories in the well, whereas the imaginary part (i.e. the decay rate Γ_n) is related to the probability current density flow from the well to the barrier.

Using the instanton approach procedure shortly described in the Sections II and III (for the details see [10], [11]), in own turn one can find not only eigen values but as well eigen states. The real-valued instanton wave functions are determined by the action $W(X_1, X)$ which is counted from the linear turning point X_1

$$\Psi(X) = A(\alpha)|X - X_1|^{-1/4}\sin(\gamma W(X_1, X) + \pi/4), \tag{4.20}$$

where the amplitude $A(\alpha)$ of the wave function acquires maximum values at the poles of (4.16) with widths proportional to Γ_n. We plotted the functions $|A(\alpha)|^2$ in Fig. 6.

V. RESONANCE TUNNELING.

The phenomenom of the electron resonance tunneling is a familiar one [27] and observed (see e.g. [28], and for more recent references also [29]) in semiconducting heterostructures possessing so-called double barrier potentials (see Fig. 8). The phenomenom manifests itself as peaks in the tunneling current at voltages near the quasistationary states of the potential well. The physical mechanism of the resonance tunneling can be understood as a constructive interference between the wave reflected from the left barrier and outgoing to the left from the well.

In the instanton method the total transmission coefficient T is determined by the second order turning points of the double barrier potential (i.e. the maxima of the potential) and according to the procedure shortly described in the Section II, T reads as

$$|T|^2 = \frac{\pi^2\Gamma_L\Gamma_R}{(1 - \sqrt{(1+\pi\Gamma_L)(1+\pi\Gamma_R)})^2 + 4\sqrt{(1+\pi\Gamma_L)(1+\pi\Gamma_R)}\cos^2(\gamma W_R^*)}, \tag{5.1}$$

where we designate

$$\Gamma_{L,R} = \frac{1}{\pi}\exp(-\pi\alpha_{L,R}), \tag{5.2}$$

as above (2.12)

$$\alpha_{L,R} = 2\frac{U_{0(L,R)} - E}{\Omega_{0(L,R)}}, \tag{5.3}$$

and the action in the classically admissible region analogously to (3.19) is

$$\gamma W_R^* = \gamma W^* - \phi(\alpha_L) - \phi(\alpha_R). \tag{5.4}$$

In the resonance region, where according to the stationary quantization rule

$$\gamma W_R^* = \pi \left(n + \frac{1}{2} \right) ,$$

the transmission coefficient from (5.1) is

$$|T|^2 = \frac{4\Gamma_L \Gamma_R}{(\Gamma_L + \Gamma_R)^2} , \tag{5.5}$$

and far from the resonance

$$|T|^2 = \frac{\pi^2 \Gamma_L \Gamma_R}{4 \cos^2(\gamma W_R^*)} . \tag{5.6}$$

Thus we found the resonance amplification of the transmission. For the symmetric case in the resonance $T = 1$, and the interference suppresses completely reflection. In the opposite case of strongly asymmetric barriers T from (5.1) is almost coincided with the transmission coefficient for the highest barrier, and an influence of the lower barrier is suppressed by the interference. In Fig.9 we show the energy dependence of T for the symmetrical structure of the barriers. The resonances become broader when the energy approaches to the potential barriers top, and disappear at higher energies (above the top). It is worthwhile to stress that the instanton solution of the resonance tunneling problem allows us to study the phenomenom in a very broad energetical region, including the states near the barriers tops.

Finally let us present the connection matrices for the found above instanton solutions. The corresponding matrix can be found as the product of two connection matrices connecting instanton solutions near the second order turning points (see (A9) and (3.20)), and the diagonal shift matrix (A6):

$$\begin{pmatrix} 2\pi \exp(\pi(\alpha_L + \alpha_R/4) \exp(i\gamma W^*) \{\Gamma[(1+i\alpha_L)/2]\Gamma[(1+i\alpha_R)/2]\}^{-1} + \exp(\pi(\alpha_L + \alpha_R)/2)(\exp(-i\gamma W^*) \\ -i\sqrt{2\pi} \exp[(3\pi(\alpha_R + \alpha_L)/8] \left(\exp(i\gamma W^*)\Gamma^{-1}[(1+i\alpha_R)/2] + \exp(-i\gamma W^*)\Gamma^{-1}[(1-i\alpha_L)/2] \right) \end{pmatrix} \tag{5.7}$$

$$\begin{pmatrix} i\sqrt{2\pi} \exp[(3\pi(\alpha_R + \alpha_L)/8] \left(\exp(i\gamma W^*)\Gamma^{-1}[(1+i\alpha_L)/2] + \exp(-i\gamma W^*)\Gamma^{-1}[(1-i\alpha_R)/2] \right) \\ 2\pi \exp(\pi(\alpha_L + \alpha_R/4) \exp(-i\gamma W^*) \{\Gamma[(1+i\alpha_L)/2]\Gamma[(1+i\alpha_R)/2]\}^{-1} + \exp(\pi(\alpha_L + \alpha_R)/2)(\exp(i\gamma W^*) \end{pmatrix}$$

Here as always we designated by W^* the action between the turning points (in this case between the second order turning points).

VI.   CONCLUSION

Our paper could be considered as a formal one, in the sense that we asked theoretical questions that most of solid state or chemical physics experimentalists would not think to ask. However, the answering of these very basic questions can be illuminating.

Let us sum up the results of our paper. Within the framework of the instanton approach we derived accurate analytical solutions for a number of 1d semiclassical problems, and checked numerically the results. As an illustration of the method we consider a simple quantum mechanical problem - penetration of a particle through the parabolic potential barrier. In this case the instanton solutions which are the asymptotics of the Weber equation are exact. The second investigated problem is related to the description of highly excited states in a double - well potential. For sake of concreteness and simplicity we study a quartic anharmonic X^4 potential. The instanton approach enables us to reproduce accurately not only asymptotic behavior but also a crossover region from single well to double wells quantization (in a contrast with the standard WKB approach which fails to describe the crossover behavior). The analogous problem for X^3 anharmonic potential is also studied, and the instanton method allows to study resonance broadening and collapse phenomena. Besides we investigated so-called resonance tunneling phenomena, interesting not only in its own right but as well playing a relevant role in many semiconducting double barrier structures. We computed as well the connection matrices, which provide a very efficient method of finding semiclassical solutions to the Schrodinger equation in potentials having several turning points. It is also useful for developing good analytical approximation.

All examples selected in our paper to illustrate the efficency of the instanton approach, belong to the fundamental problems of chemical dynamics and molecular spectroscopy (see e.g. the monography [9] and references herein). Symmetric or slightly asymmetric double-well potentials are characteristic for molecules and Van der Waals complexes

with more than one stable configurations [14], [15], [16], [17]. The states of such systems closed to the barrier top (theoretically described by the instanton approach in our paper) are not easy to investigate experimentally, since optical transitions between these states and localized ones, are typically inactive. However just these states are most relevant for radiationless evolution of highly excited states. In a certain sense these states have a double nature (localized - delocalized) and the nature manifests itself in the form of wave functions which contain simultaneously the both components: localized in one from the wells, and delocalized between the both of the wells. As a consequence of it, any initially prepared localized state will evolve via formation and decay of these states. Our calculations are intended to pave a way to investigate this class of problems using the wave functions computed within the instanton approach.

The states close to the barrier top of decay potentials govern of thermally activated over-barrier transition amplitudes. For the low energy states the main reduction factor is the tunneling exponent, while the contribution of the highly excited states is limited by the Boltzmann factor. The energetical width of the region dominating in the total transition rate is postulated traditionally in the transition rate theory [31] as being of the order of the temperature T. However our results presented in the Section III predict another estimation. Instanton calculations demonstrate that the intermediate region between the quasistationary $\Gamma \ll \Omega$ and delocalized states could be much larger than T, namely of the order of Ω. It means that there is no sharp boundary between quasistationary and delocalized states and all of the states within the interval $V^* - \Omega$, $V^* + T$ equally contribute to the total rate constant for the penetration through the barrier.

One more point should be emphasised. Recently in [18] has been shown that quantum irreversibility phenomena occur when the spacing between neighbouring levels of a deeper well becomes smaller than the typical transition matrix element. Obviously this criterion can be also applied to the states near the barrier top. Note that for the low energy states the asymmetry providing irreversible behavior should be very large, whereas for the states near the barrier top, the condition to have the ergodic behavior is not so severe, it is sufficient that the asymmetry of the potential is comparable to the barrier height.

Applications of the method and of the results may concern also the various systems in physics, chemistry and biology exhibiting double level behavior and resonance tunneling. Literally speaking in this paper we dealt with the microscopic Hamiltonians. However, thanks to the rapid development of electronics and cryogenic technologies, it has become possible to apply the same Hamiltonians to study cases where the corresponding variables are macroscopic (e.g. magnetic flux through a SQUID ring, or charge or spin density waves phase in a certain one dimensional solids). For example in the paper we studied tunneling processes in which a system penetrates into a classically forbidden region (a potential barrier). It is an intrinsically quantum effect with no classical counterpart, but nevertheless it can take place for macroscopic systems, and the tunneling of a macroscopic variable of a macroscopic system (e.g. spin or charge tunneling in atomic condensates trapped in a double-well potential [32]) can be also investigated by our method.

With this background in mind our results are also intended to clarify different subtle aspects of tunneling phenomena. An example was given at the end of the Section III , where we found the geometrical phase acquired by a particle tunneling through a potential barrier. This phase can be tuned by the particle energy and by the barrier shape, and specific interference phenomena might occur. The observation of oscillations related to this geometrical phase in real systems has proved challenging. Of course since the forms of the model potentials we used are rather specialized (and besides only 1d), we cannot discuss the behavior for general cases with full confidence. Nevertheless, we believe that the instanton approach employed in the present work should be useful in deriving valuable results for the general and multidimensional potentials as well.

Essentially that in the instanton method, we discussed in the paper, just observing a few classical trajectories suffices to develop a qualitative insight for quantum behavior. Though (as we illustrated in a number of particular examples considered in the paper) relied upon in this way, semiclassical instanton approach is much more than a qualitative picture. As an approximation, the instanton method can be surprisingly precise. Note also that results presented here not only interested in their own right (at least in our opinion) but they might be directly tested experimentally since there are many systems where the model investigated in the paper is a reasonable model for the reality.

The theory presented in our paper could be extended in several directions. One very interesting question is how our quantum mechanic instanton formulas (e.g. (4.12) - (4.14) for the tunneling rate in the anharmonic X^3 decay potential) are modified by interactions with surrounding media (see e.g. [30], where WKB approach was used to study the time evolution of quantum tunneling in a thermally fluctuating medium). However the theoretical modelling of this case is hampered by lack of detailed knowledge of the medium and of the interaction with it. A more specific study might become appropriate should suitable experimental results become available. A simple criterion for the strength of interaction with an environment (or by other words for the effective temperature) where roughly the crossover from thermally activated classical to quantum mechanical decay can be found easily by equating the corresponding Arrhenius factor and characteristic frequency "oscillations" inside the barrier Ω_* (see (A10)).

All of the potentials investigated in our paper can be considered in a number of realistic cases as effectively resulting

from avoiding of adiabatic level crossing in the situation, when the adiabatic splitting is so large that any influence of the upper adiabatic states on the lower states can be neglected. Certainly in a general case of an arbitrary coupling strength, this interaction of higher and lower adiabatic states must be taken into account, and the tunneling matrix elements are accompanied by corresponding Franck - Condon factors arising due to violation of Born Oppenheimer approximation. We defer these problems to the further, although no any doubt the instanton approach is useful for this kind of problems as well.

Acknowledgments

APPENDIX A

For the standard basic WKB solutions following [2] we will introduce shorthand notations

$$(\circ, z) \equiv (q(z))^{-1/4} \exp(i\gamma W(z)), \tag{A1}$$

and

$$(z, \circ) \equiv (q(z))^{-1/4} \exp(-i\gamma W(z)), \tag{A2}$$

The position of the turning point is designated by $\circ$ and not essential if we are looking for the solutions in the region $|z| \gg 1$. According to the definitions (2.18), (2.19) on the Stokes lines one should add the dominant solution times a certain constant (Stokes constant) to the subdominant (decaying) solution, while on the anti-Stokes lines the dominant and the subdominant solutions are exchanged. To find the Stokes constant we must match the both solutions going around the turning point and taking into account the cut on the complex z plane (see Fig. 10).

Let us consider first the linear turning point

$$q(z) = -z, \tag{A3}$$

when the classically admissible region corresponds to $X > 0$. For this case we have 3 Stokes lines, 3 anti-Stokes lines, one cut, and therefore 7 different regions on the complex z-plane where the functions (A1), (A2) should be matched, and after that 3 Stokes constant should be determined. After not very sophisticated but rather tedious algebra we are ending with all three Stokes constants

$$T_1 = T_2 = T_3 = i,$$

and the connection matrix related the coefficients of the combinations of the basic solutions (A1), (A2) in the classically are ending (A_1, A_2) and in classically admissible (A_2, B_2) regions are

$$\begin{pmatrix} A_2 \\ B_2 \end{pmatrix} = \hat{M}^- \begin{pmatrix} A_1 \\ B_1 \end{pmatrix} \tag{A4}$$

where

$$\hat{M}^- = \exp\left(-i\frac{\pi}{4}\right) \begin{pmatrix} \exp(i\pi/4) & (1/2)\exp(-i\pi/4) \\ \exp(-i\pi/4) & (1/2)\exp(i\pi/4) \end{pmatrix} \tag{A5}$$

Analogously for the other linear turning point $q(z) = +z$, the connection matrix $\hat{M}^+$ is Hermitian conjugated to $\hat{M}^-$. The variation of the coefficients in the region between two independent linear turning points z_1 and z_2 are determined by the diagonal matrix $\hat{L}$

$$\hat{L} = \begin{pmatrix} \exp(-i\gamma W^*) & 0 \\ 0 & \exp(+i\gamma W^*) \end{pmatrix} \tag{A6}$$

where

$$W^* = \int_{z_1}^{z_2} \sqrt{q(z)} dz.$$

And finally for the solutions in the classically forbidden regions $X < X_1$ and $X > X_2$ the connection matrix is the direct matrix product of the found above matrices

$$\hat{M} = \hat{M}^+ \hat{L} \hat{M}^- .$$

To generalize the procedure for the second order turning points we should find the connection matrices related the basic solutions to the Weber equation, namely

$$(\circ, z) \equiv (z)^\nu \exp(-z^2/4) , \tag{A7}$$

and

$$(z, \circ) \equiv (z)^{-\nu-1} \exp(z^2/4) . \tag{A8}$$

In this case we have 4 Stokes lines, 4 anti-Stokes lines, one cut, and therefore 9 different regions, where the solutions should be matched (see Fig. 11a as an illustration). Four Stokes constants are

$$\tilde{T}_1 = \tilde{T}_2^{-1}(\exp(i2\pi\nu) - 1) , \, \tilde{T}_3 = \tilde{T}_1^* , \, \tilde{T}_4 = -\tilde{T}_2 \exp(-i2\pi\nu) .$$

And from the known asymptotic of the parabolic cylinder functions one can get the last remaining Stokes constant

$$\tilde{T}_2 = \frac{\sqrt{2\pi}}{\Gamma(-\nu)} .$$

Thus the connection matrix for an isolated second order turning point can be represented as

$$\begin{pmatrix} -\tilde{T}_2 & \cos(\pi\nu) \\ \cos(\pi\nu) & -\sin^2(\pi\nu)/\tilde{T}_2 \end{pmatrix} \tag{A9}$$

For example this depending on the energy ϵ matrix determines instanton semiclassical solutions for the harmonic oscillator $\epsilon = \nu + 1/2$. It can be checked by explicit calculations that for the harmonic oscillator the same form (A9) of the connection matrix holds as well for WKB approach. The difference could appear only from anharmonic terms in the potential. However for low energy states $\epsilon/\gamma \ll 1$ anharmonic corrections are small and up to the second order over these corrections terms the both connection matrices (instanton and WKB) coincide.

The connection matrix describing the variation of the coefficients at the basic solutions (A7), (A8) between two second order turning points X_2^0 and X_3^0 for the symmetrical double-well potential is (compare with the analogous matrix (A6) for two linear turning points)

$$\begin{pmatrix} (n!/\sqrt{2\pi})(\Omega_0\gamma/\Omega_*)^{-\nu+1/2} \exp(\gamma W_E^*) & 0 \\ 0 & (\sqrt{2\pi}/n!)(\Omega_0\gamma/\Omega_*)^{\nu+1/2} \exp(-\gamma W_E^*) \end{pmatrix} \tag{A10}$$

where the instanton action

$$W_E^* = \int_{X_2^0}^{X_3^0} \sqrt{2(V(X) - (\epsilon/\gamma))} dX , \tag{A11}$$

and Ω_* is the characteristic "oscillation" frequency in the barrier (i.e. in the classically forbidden region). For the asymmetric double-well potential in the region between the second order and the linear turning points the analogous to (A10) matrix is

$$\begin{pmatrix} (n!/\sqrt{2\pi})^{1/2}(\Omega_0\gamma/\Omega_*)^{-(1/2)(\nu+1/2)} \exp(\gamma W_E^*) & 0 \\ 0 & (\sqrt{2\pi}/n!)^{1/2}(\Omega_0\gamma/\Omega_*)^{(1/2)(\nu+1/2)} \exp(-\gamma W_E^*) \end{pmatrix} \tag{A12}$$

All given above matrices allow us to find any other connection matrices we need for all particular examples considered in the main text of the paper. Any of them can be constructed as a corresponding product of (A4), (A5), (A6), (A9), (A10), (A12). It is worth noting at the very end one general property of the connection matrices, namely that for all bound states the connection matrix is real-valued, and for continuum spectrum states, off-diagonal elements of the connection matrix are complex.

Analogously for the problem of tunneling through the potential barrier $V(X) = -(1/2)X^2$, all Stokes and anti-Stokes lines are turned by the angle $\pi/4$ (see Fig. 11b) with respect to the corresponding lines for the parabolic well $(V(X) = (1/2)X^2$ considered above, see Fig. 11a). The connection matrix for the tunneling through the barrier

$$\begin{pmatrix} (S_1 & -i\exp(\pi\alpha/2) \\ i\exp(\pi\alpha/2) & S_1^{-1}(\exp(\pi\alpha) + 1) \end{pmatrix} \tag{A13}$$

where $\alpha = i(2\nu + 1)$ and S_1 is the Stokes constant on the first quadrant bisectrix (see Fig. 11b). To find the Stokes constant S_1 one has to match the sum of the incident and of the reflected waves to the solutions of the Weber equation at $X \to -\infty$ and to the transmitted wave at $X \to \infty$. It leads

$$S_1 = \frac{\sqrt{2\pi}}{\Gamma[(1 + i\alpha)/2]} \exp(\pi\alpha/4).$$

[1] L.D.Landau, E.M.Lifshits, Quantum Mechanics (non-relativistic theory), Pergamon Press, New York (1965).
[2] J.Heading, An Introduction to Phase-Integral Methods, Wiley - Interscience, London (1962).
[3] V.L.Pokrovskii, I.M.Khalatnikov, JETP, **13**, 1207 (1961).
[4] N.T.Maintra, E.J.Heller, Phys. Rev. A, **54**, 4763 (1996).
[5] C.S.Park, M.C.Jeong, Phys. Rev. A, **58**, 3443 (1998).
[6] A.K.Roy, N.Gupta, D.M.Deb, Phys. Rev. A, **65**, 012109 (2002).
[7] A.M.Polyakov, Nucl.Phys. B, **129**, 429 (1977).
[8] S.Coleman, Aspects of Symmetry, Cambridge University Press, Cambridge (1985).
[9] V.A.Benderskii, D.E.Makarov, C.A.Wight, Chemical Dynamics at Low Temperatures, Willey-Interscience, New York (1994).
[10] V.A.Benderskii, E.V.Vetoshkin, H.P.Trommsdorf, Chem. Phys., **244**, 273 (1999).
[11] V.A.Benderskii, E.V.Vetoshkin, Chem. Phys., **257**, 203 (2000).
[12] V.A.Benderskii, E.V.Vetoshkin, L.S.Irgebaeva, H.P.Trommsdorff, Chem. Phys., **262**, 369 (2000).
[13] I.M.Lifhsits, Yu.Kagan, JETP, **35**, 206 (1972).
[14] M.Grifoni, P.Hanggi, Phys. Repts., **304**, 229 (1998).
[15] J.E.Avron, E.Gordon, Phys. Rev. A, **62**, 062504 (2000).
[16] J.Ankerhold, H.Grabert, Europhys. Lett., **47**, 285 (1999).
[17] Y.Kaganuma, Y.Mizumoto, Phys. Rev. A, **62**, 061401(R) (2000).
[18] V.A.Benderskii, E.I.Kats, Phys. Rev. E, **65**, 036217 (2002).
[19] V.V.Avilov, S.V.Iordanskii, JETP, **69**, 1338 (1975).
[20] V.A.Benderskii, E.V.Vetoshkin, L. von Laue, H.P.Trommsdorff, Chem. Phys., **219**, 143 (1997).
[21] A.M.Dykhne, JETP, **14**, 941 (1961).
[22] A.Erdelyi, W.Magnus, F.Oberhettinger, F.G. Tricomi, Higher Transcendental Functions, vol.1 - vol.3, McGraw Hill, New York (1953).
[23] M.Berry, Proc. Roy. Soc. London, ser. A, **392**, 45 (1984).
[24] M.Wilkinson, J.Phys. A, **17**, 3459 (1984).
[25] H.Karatsuji, Progr. Theor. Phys., **74**, 439 (1985).
[26] A.O.Caldeira, A.J.Legget, Ann. Phys., **149**, 374 (1983).
[27] D.Bohm, Quantum Theory, Englewood Clifs, New Jersy (1951).
[28] L.L.Chang, L.Esaki, R.Tsu, Appl. Phys. Lett., **24**, 593 (1974).
[29] J.P.Eisenstein, L.N.Pfeiffer, K.W.West, Phys. Rev. Lett., **74**, 1419 (1995).
[30] Sh.Matsumoto, M.Yoshimura, Phys. Rev. A, **63**, 012104 (2000).
[31] M.Baer, Phys. Repts., **358**, 75 (2002).
[32] H.Pu, W.Zhang, P.Meystre, Phys. Rev. Lett., **87**, 140405 (2001).

Figure Captions.

Fig. 1

The phase of the reflected from the parabolic barrier wave:

(1) - exact quantum and instanton solutions ϕ_0;

(2) - WKB solution ϕ_0^{WKB};

dashed line is the difference $\phi_0 - \phi_0^{WKB}$.

Fig. 2

The Stokes (solid) and anti-Stokes (dashed) lines for the two real-valued turning points $X_{1,2}$ with the surrounding contours I and I'. On the contour II the Stokes lines for the Airy equation asymptotically matched to the lines for the Weber equation. The cut is depicted by the wavy line.

Fig. 3

The same as Fig. 2 but for the case of the two pure imaginary turning points $iX_{1,2}$.

Fig. 4

The dimensionless tunneling splitting Δ/Ω_0 for the anharmonic X^4 potential near the barrier top:

(1) - exact quantum and instanton calculations;

(2) - WKB result.

Fig. 5

The X^3 anharmonic decay potential.

Fig. 6

The amplitude of the wave function localized in the potential shown in Fig. 5 (the dashed line is a non-resonant part of the amplitude, and $\gamma = 101$).

Fig. 7

The model two barrier potential structure for the resonance tunneling.

Fig. 8

The transmission coefficient for the potential shown in Fig. 7 ($\gamma = 54$).

Fig. 9

The Stokes (solid) and anti-Stokes (dashed) lines in the vicinity of the linear turning point $V(X) = -X$. The cut is depicted by the wavy line, and the Stokes constant are T_1, T_2, and T_3.

Fig. 10

The Stokes and anti-Stokes lines in the vicinity of the second order turning points (the same notations as in the Fig. 9):
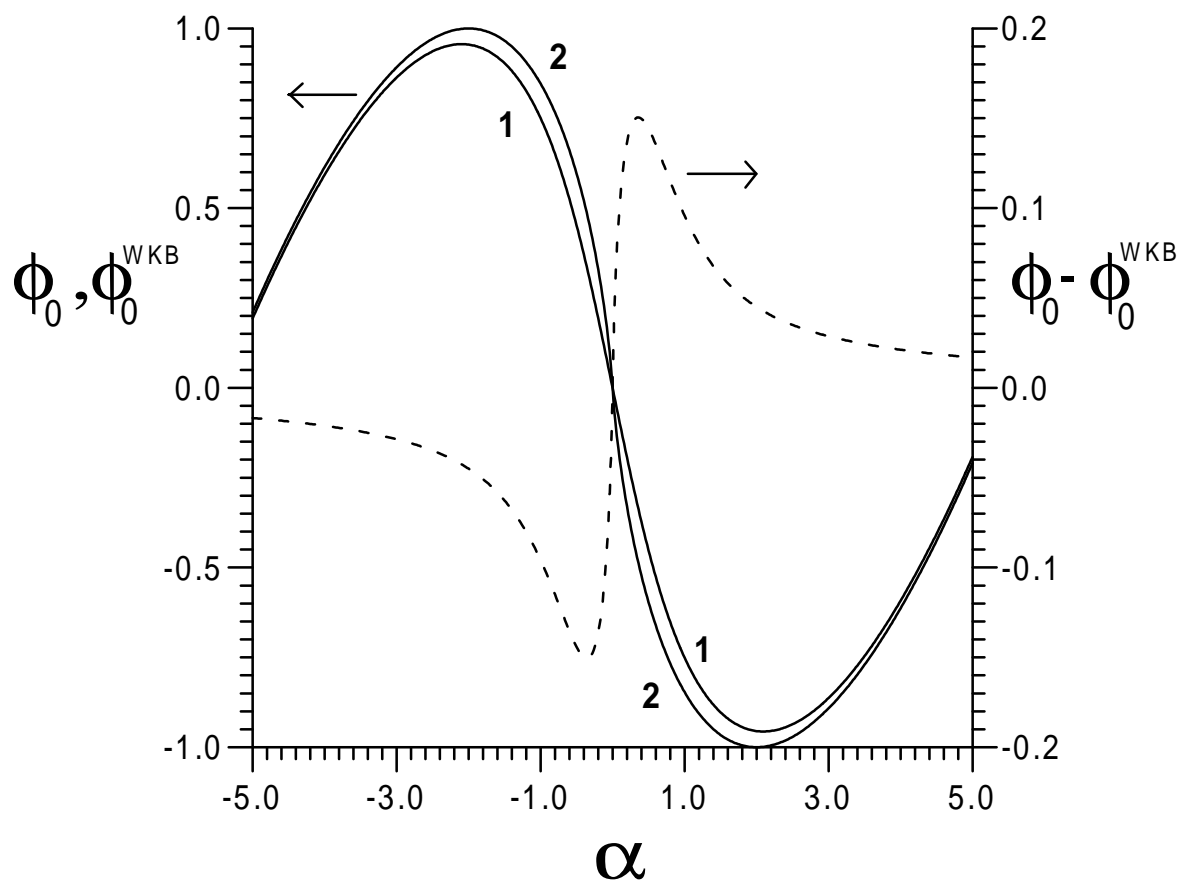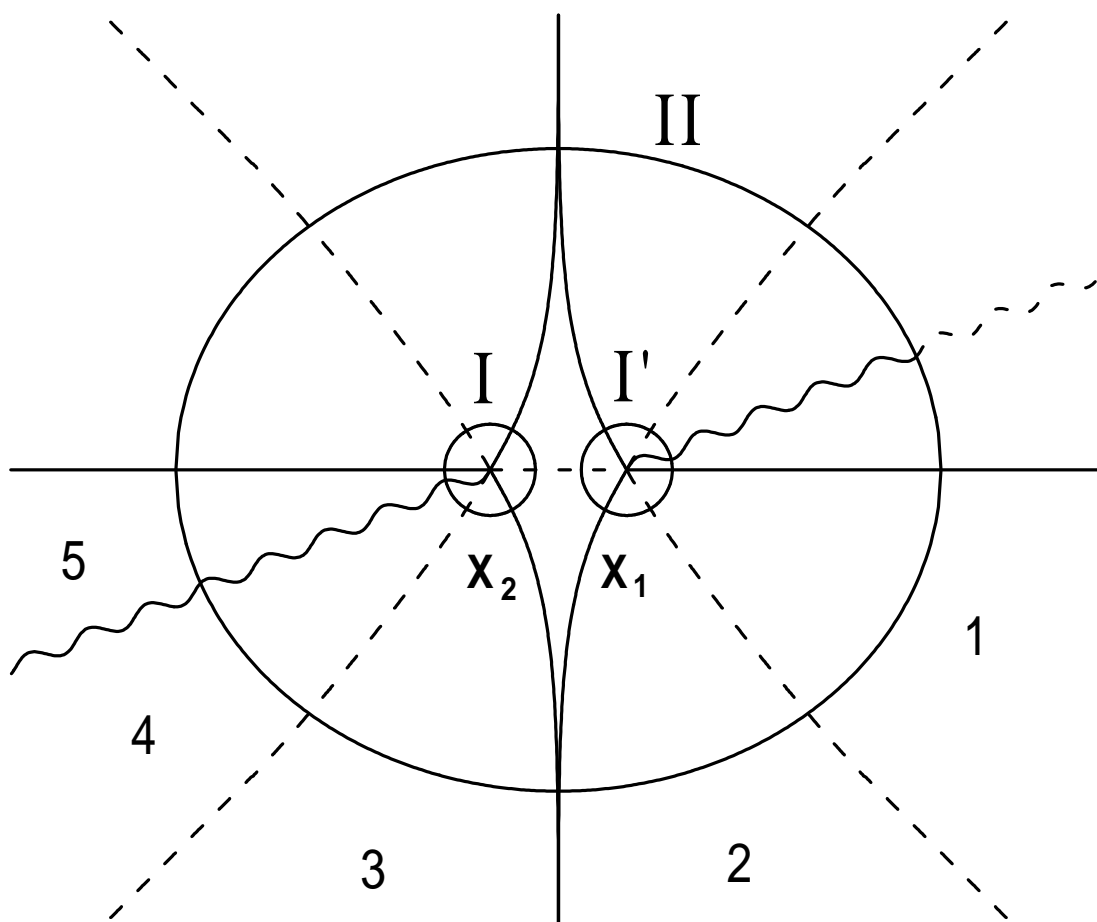
(a) $V(X) = (1/2)X^2$;

(b) $V(X) = -(1/2)X^2$.

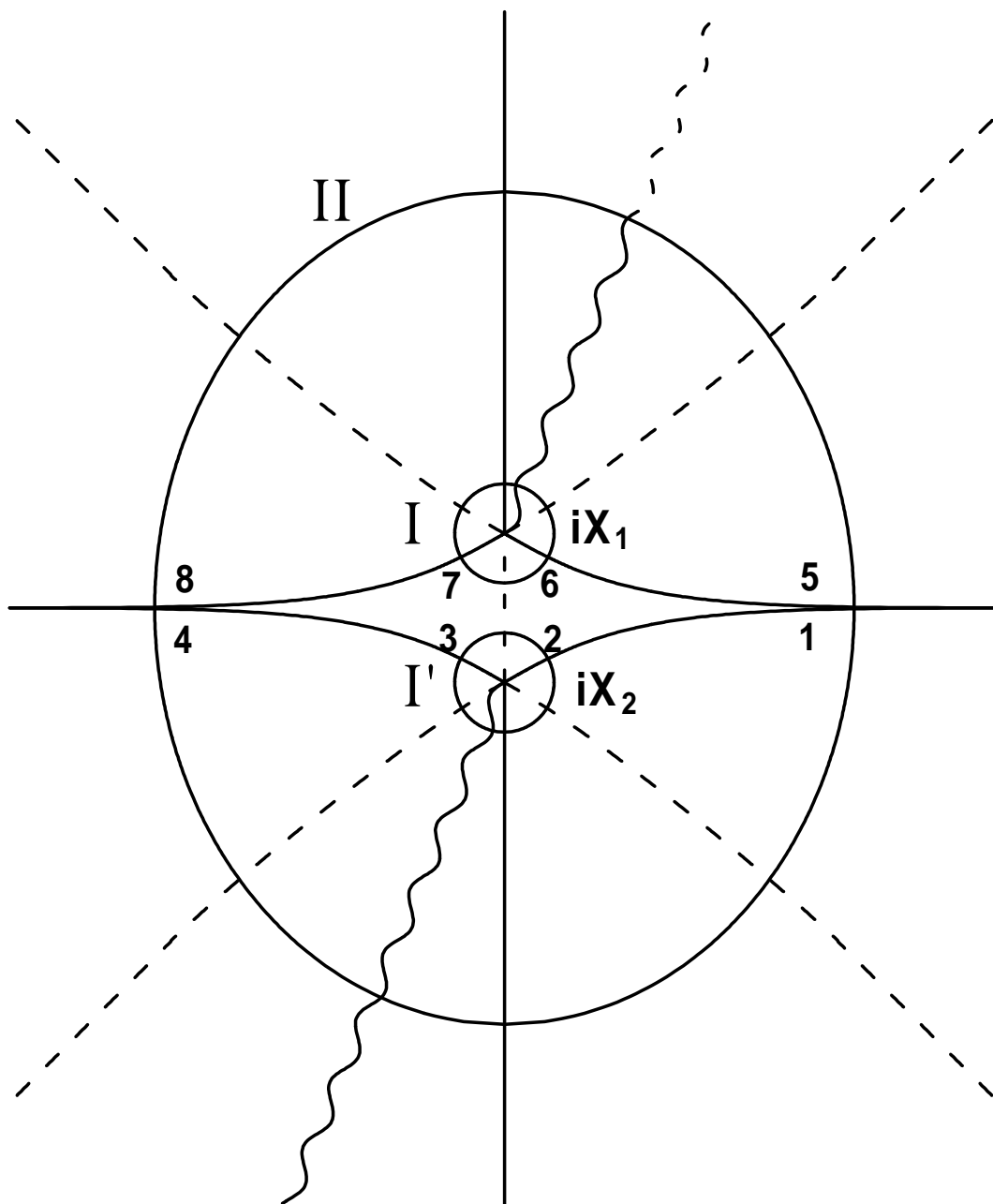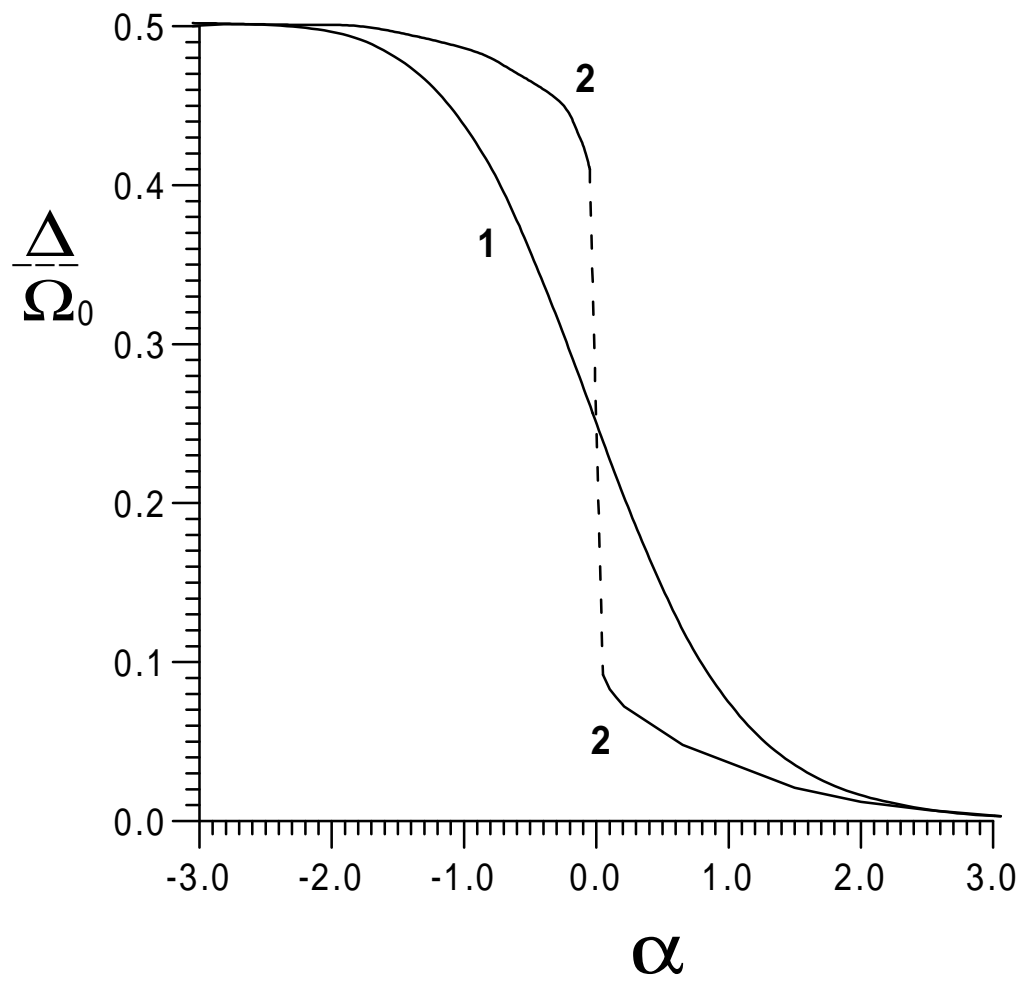ϕ_0, ϕ_0^{WKB}

$\phi_0 - \phi_0^{WKB}$

α

2

1

1

2

1.0

0.5

0.0

-0.5

-1.0

0.2

0.1

0.0

-0.1

-0.2

-5.0   -3.0   -1.0   1.0   3.0   5.0

Fig. 1

Fig. 2

Fig. 3

Fig. 4
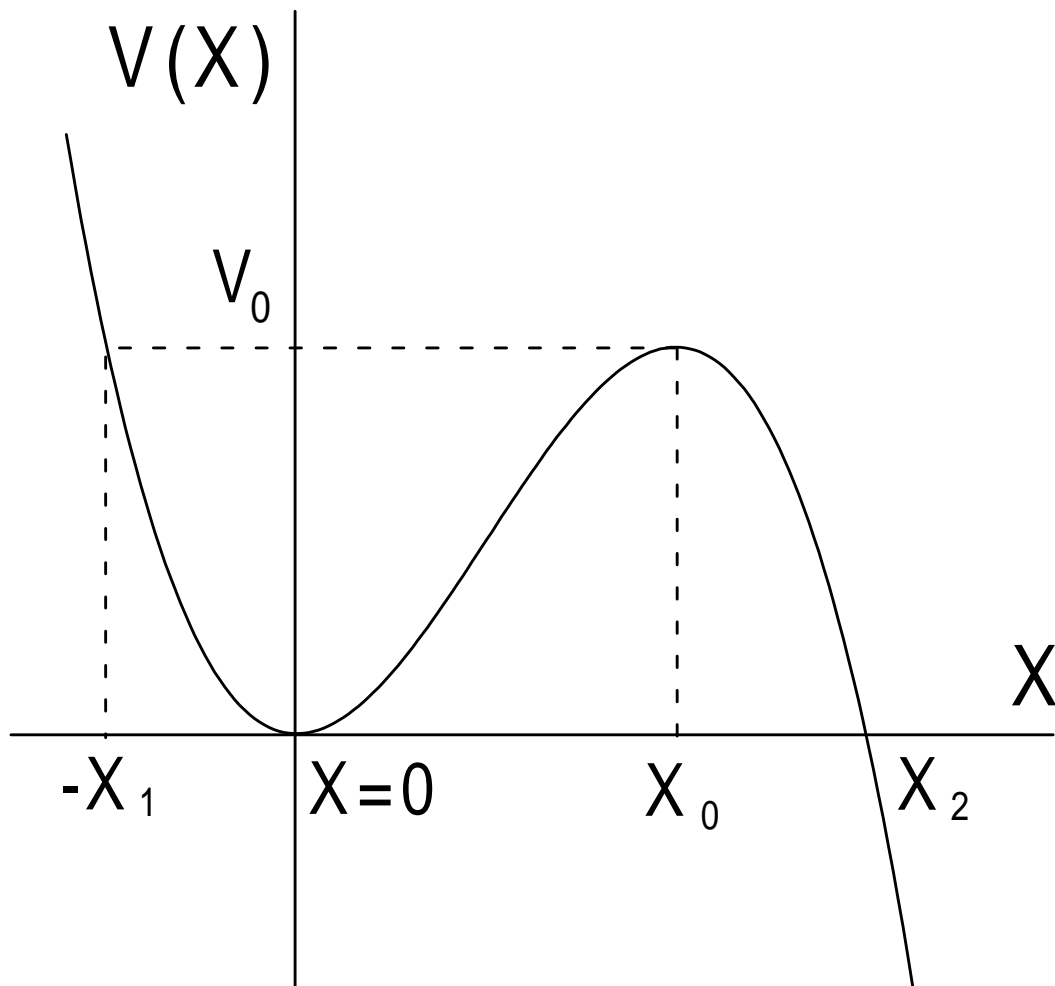
Fig. 5

Fig. 6

Fig. 7

Fig. 8

Fig. 9

a)

$\tilde{T}_2$

3   2

4   1

$\tilde{T}_3$ $\tilde{T}_1$

5

9

6

7   8

$\tilde{T}_4$

b)

$\tilde{T}_2$ $\tilde{T}_1$

3   2

4   1

5

9

6

7   8

$\tilde{T}_3$ $\tilde{T}_4$

Fig. 10